

Influence of filtering size on results in interpretation of Hopkinson-Kolsky bar signals

Rumen Krastev, Tatiana Simeonova, Vasil Kavardjikov
 Institute of Mechanics - Bulgarian Academy of Science, Sofia, Bulgaria
 R_krastev@imbm.bas.bg

Abstract: The influence of registered signals smoothing on the calculated diagram of the test specimen was analysed for impact test using split Hopkinson-Kolsky pressure bar. Two methods are used to smooth the signals: low-pass filtering built into the software and arithmetic mean averaging. When determining the elastic modulus and the upper yield stress in these high-strain rate tests, it is concluded that more accurate values are obtained by filtering with a cut-off frequency in the range of 60 to 80 kHz. For the second method, it is concluded that it is best to average the curves with an amplitude of 3 or 4 microseconds. Attention is paid to the correct choice of the initial moments from which the reading of the signals begins because the wrong choice leads to inaccurate calculations and conclusions about the properties of the tested material.

Keywords: SPLIT HOPKINSON-KOLSKY PRESSURE BAR, SIGNALS, FILTERING, DATA TREATMENT

1. Introduction

At the beginning of 2021, in implementation of a project BG05M2OP001-1.001-0008 "National Center for Mechatronics and Clean Technologies", a new experimental equipment was installed at the Institute of Mechanics at the Bulgarian Academy of Sciences – Split Hopkinson-Kolsky Pressure Bar (Fig. 1). This device is used for determination of materials properties at high deformation rates. It applies a load to the test specimen similar to that which the material would withstand in real situations like car accidents or other high-energy collisions. Modern implementations of these devices are used to study metals and metal alloys [1-4], concrete, foam concrete and reinforced concrete with different fibres [5-12], geological materials (marble, rocks) [13, 14], different 3D printing materials and products made by this technology [15, 16] and composite materials [17]. In addition to experiments with compressive impact deformation along the sample axis, shear deformation can also be realised [18]. Often modern devices of this type are equipped with high-speed cameras, which visualise the process of shock deformation, and/or determine the field of deformation of the observed surface of the sample by correlation analysis of the recorded images [19]. The results obtained from these measurements provide essential information about the properties of the tested materials for scientific and engineering applications. Researchers use them as input data in developing numerical models of structures from relevant materials and in basic research related to defining constitutive equations describing the behaviour of materials under dynamic loading [20].

Experiments are conducted by mounting a cylindrical test body between two rods, called *Incident Bar* (IB) and *Transmitted Bar* (TB). Strain gauges are glued in the middle of the two bars, and the machine is equipped with a computer and a recording device for the signals coming from these strain gauges.

There is a theoretical model for determining the compressive stress and strain of the crushed specimen, which uses the registered strain pulses in time.

The registered signals *strain-time* have fluctuations that affect the quality of the determined diagrams. To improve the results, a low-pass software filter is applied to the registered signals.

Accumulating experience, it became clear that the selected cut-off frequency of the filter not only smooths the resulting diagrams but also changes the slope of the observed mechanical diagram.

In this report, we analyse the influence of the selected cut-off filter frequency on the final shape of the obtained diagram (with the same output signals for all analyses). The aim is to find such cut-off frequency that will provide sufficient smoothing of the desired diagram and will have only a slight effect on its initial slope.

2. Test equipment, material and experimental plan

A pressure Hopkinson's bar, as modified by Kolsky (Fig. 1), contains a launching device (1) powered with compressed air. It can fire strikers at planned speed. The available strikers are 200 to 800 mm long and have a diameter of 20 mm, the same as the diameter of the main bars. After firing the selected striker, its impulse is passed to the incident bar (2), creating in it a longitudinal pressure wave that moves at the speed of sound. The test specimen (4) is deformed between the IB and the transmitted bar (5), as part of the impact wave is reflected (from the end of the bar 2) and is registered through the strain gauges (3), and another part is transmitted through the test specimen and is registered by the strain gauges (6), located in the middle of the TB (5). Behind the last rod (7), there are devices (not visible in Fig. 1) for suppressing the movement after impact. The equipment works well when the system of bars are positioned with minimal deviations from a straight line.



Fig. 1 Split Hopkinson-Kolsky pressure bar

1- Launching device, 2-Incident bar, 3-Strain gauges in the middle of IB, 4- Test piece, 5-Transmitted wave bar, 6- Strain gauges in the middle of TB, 7- motion suppression bar.

IB and TB are made of "Maraging 300" steel with a diameter of 20 mm and a length of 2000 mm. A striker with 600 mm length was used for this experiment. There are disk anvils of the same diameter and 8 mm length on both sides of the test specimen. On the forehead of the incident bar is used a shaper - washer M4 according to DIN 9021 made of A2 steel.

The influence of filtering on the obtained results will be shown by processing the signals from one of the tests in different ways. The test specimen is made of duralumin with initial dimensions: 5 mm diameter and 5 mm length. The speed of the striker before the impact with the IB is estimated as 13.3 m/s.

The experimental plan is expressed in signal processing and analysis of the results, as smoothing of the signals is done in different sizes and by two methods:

- Using the built-in filter, at the following cut-off frequencies: 40, 60 and 80 kHz.
- Using the averaging method described in section 3.4, at the following averaging amplitudes: 1, 2, 3, 4, 6, 8, 10 and 12 microseconds.

The results obtained without any signal smoothing are compared with the results obtained after smoothing.

3. Signal processing methods

3.1 Simplified analytical model

The mechanical diagram of the test specimen for the described Hopkinson-Kolsky bar is obtained by the following "simplified" system of equations [21, 22]:

$$\dot{e}_s(t) = \frac{-2c_b}{l_0} \varepsilon_R(t) \quad (1)$$

$$e_s(t) = \int_0^t \dot{e}_s(\tau) d\tau \quad (2)$$

$$s_s(t) = E_b \frac{A_b}{A_{s0}} \varepsilon_T(t) \quad (3)$$

Where:

t – Time

$\varepsilon_R(t)$ – Reflected (by the end of IB) signal

c_b – Propagation velocity of the deformation waves (pulses) in the bars, 4730 m/s

l_0 – Initial sample length

$\dot{e}_s(t)$ – Sample deformation rate

$e_s(t)$ – Nominal (engineering) deformation of the sample, calculated for moment t

$\varepsilon_T(t)$ – Passed through the sample (transmitted) deformation pulse

E_b – Elastic modulus of all bars, 181 GPa.

A_b – Cross-section of the bars

A_{s0} – Initial cross-section of the sample

$s_s(t)$ – Nominal (engineering) stress in the sample for moment t .

It is accepted that stress and strain are considered as positive values even though the sample is subjected to compression [22]. Therefore, the signs of the recorded signals must be reversed.

During an impact deformation of the sample, its dimensions change significantly. Therefore, under compression and while the variables are positive, the true strain ε_s and the true stress σ_s are calculated by the formulas (4) – (6), [22]:

$$\varepsilon_s(t) = -\ln[1 - e_s(t)] \quad (4)$$

$$\dot{\varepsilon}_s(t) = \frac{\dot{e}_s(t)}{1 - e_s(t)} \quad (5)$$

$$\sigma_s(t) = s_s(t)[1 - e_s(t)] \quad (6)$$

3.2 Start of signal reporting

The recorded signals are available in tabular form, every 1 microsecond. Before mathematical processing, the starting points in time must be chosen for both signals (reflected and transmitted). The machine is designed so that these two points coincide or at least be close enough to each other.

Our experience has shown that beginning of the signal $\varepsilon_T(t)$ is delayed by about 13 μ s after the beginning of the signal $\varepsilon_R(t)$, as shown in Fig.2. We think this is due to the passage of the strain pulse through the sample and by removal of gaps between the sample, disk anvils and bars.

To obtain quality results, it is crucial the starting points of reading the signals $\varepsilon_R(t)$ and $\varepsilon_T(t)$ to be chosen correctly, using a theoretically and empirically justified method. In the presented calculations and results, the starting moments of reading the two signals were chosen to be (approximately) when $|\varepsilon_R(t)| = 10/100 * \max(|\varepsilon_R|)$ and $\varepsilon_T(t) = 10/100 * \max(\varepsilon_T)$.

3.3 Signal filtering

The experimental equipment is provided with a computer and signal processing software developed by the manufacturer - THIOT INGENIERIE. The software contains an option for signals filtering where a "threshold frequency" is selected. In subsequent calculations, the software uses the filtered curves (Fig. 3).

3.4 Signal smoothing by averaging

The recorded signals are available in tabular form through 1 μ s. The aim is to suppress unwanted signal fluctuations by averaging adjacent values. Select the *amplitude of averaging* A , μ s, and determine *averaging period and frequency*.

$$T = 2A \quad \mu\text{s}, \quad (7)$$

$$\nu = \frac{1}{T} \quad \text{Hz}, \quad (8)$$

Example: $A = 12 \mu$ s; $T = 2A = 24 \mu$ s. $\nu = 1/(24 \cdot 10^{-6}) = 41.7$ kHz. These parameters were introduced for comparison with the threshold frequency of the other method (section 3.3).

Formulas for smoothing signals and inverting signs

$$\bar{\varepsilon}_R(t) = -\text{Average} \varepsilon_R \left(\frac{t-A}{t+A} \right) \quad (9)$$

$$\bar{\varepsilon}_T(t) = -\text{Average} \varepsilon_T \left(\frac{t-A}{t+A} \right) \quad (10)$$

The function *Average* in Excel software is used to find the mean value at moment t , as the arithmetic mean of the values in the range from $t-A$ to $t+A$ inclusive. When processed in Excel tables, the time increases from top to bottom and, therefore, in Eqs. (9) and (10), the later value of the interval is written below. Index R refers to reflected pulse, and index T refers to the strain pulse transmitted through the sample. In Eqs. 9 and 10, the minus sign satisfies the requirement for stress and strain to be positive in subsequent calculations.

4. Experimental result and discussion

4.1 Recorded signals

The reflected strain pulse and the strain pulse passed through the sample are shown in Fig. 2. The duration corresponds to the 600 mm striker used, and the pulse shape is typical for the used shaper.

Several sharp pulsations of the signals are visible, the most drastic at the moment being 594 μ s. These ripples affect 1 to 2 adjacent recorded values. The filtration techniques are mainly used to suppress such pulsations, which are not a property of the material under study, but have an electrical origin.

Before starting the calculations in accordance with Eqs. (1) - (6), the beginning points in the time must be selected, for both signals. The points when $\varepsilon_R(t) = 77 \mu\text{m/m}$ and $\varepsilon_T(t) = -27 \mu\text{m/m}$ were selected, and they are indicated in Fig. 2. The difference between them is 13 μ s.

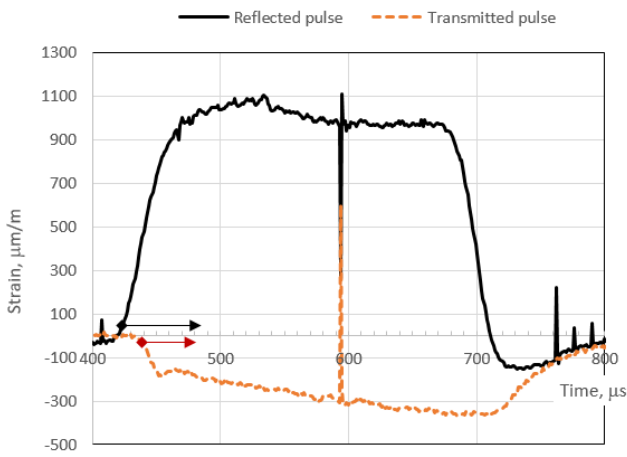


Fig. 2 Recorded signals

4.2 Smoothed signals

Figs. 3 and 4 show the signals smoothed by the two mentioned methods: with the built-in the machine’s software low-pass filter at a threshold frequency of 40 kHz, and by averaging as described in section 3.4, at $A = 12 \mu s$.

The curves are visualised from the selected start times. It can be seen that the curves are smoothed similarly, but differences show that mathematical apparatuses of both methods are different.

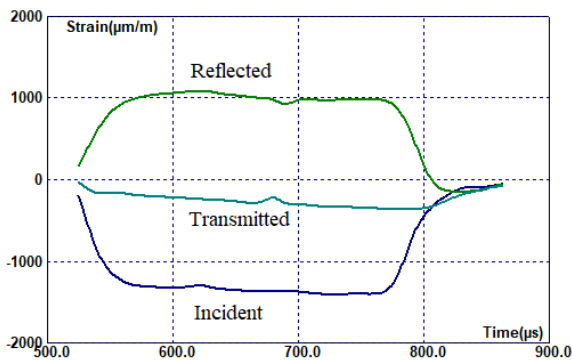


Fig. 3 Filtered signals, threshold frequency = 40 kHz.

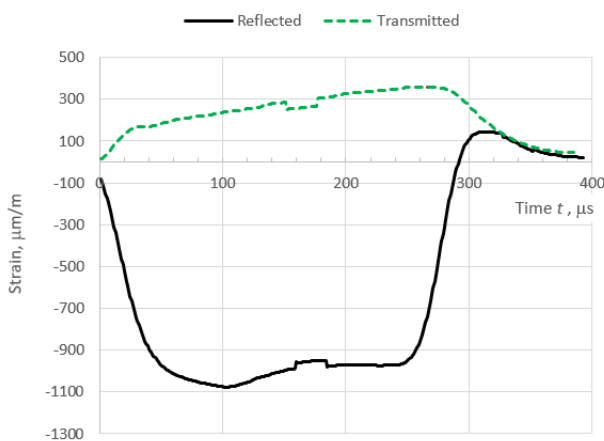


Fig. 4 Averaged and reversed signals, $A = 12 \mu s$.

4.3 Influence of the size of filtering (averaging) on the final diagram

Figure 5 shows how the selected cut-off frequency of the low-pass filter affects the calculated mechanical diagram.

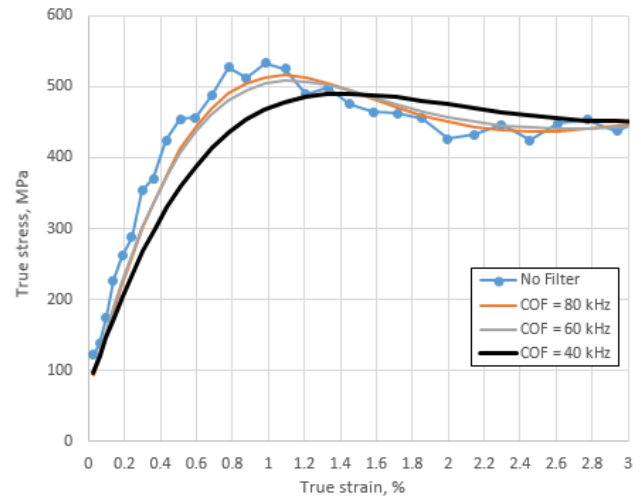


Fig. 5 Diagrams of the test sample, calculated with the original equipment software at different sizes of filtration (cut-off frequencies: 40, 60 or 80 kHz).

Fig. 5 shows that a filter with 40 kHz cut-off frequency has a noticeable effect on the initial slope of the curve and the upper yield strength. The reduction is 30% for the elastic modulus and 8% for the upper yield strength.

The elastic modulus is determined according to the average slope of the calculated curve for strain up to 0.2%.

The diagram obtained at 80 kHz is quite close to the raw diagram (obtained without filtering). The reduction in this case is 15% for the elastic modulus and 3% for the upper yield strength.

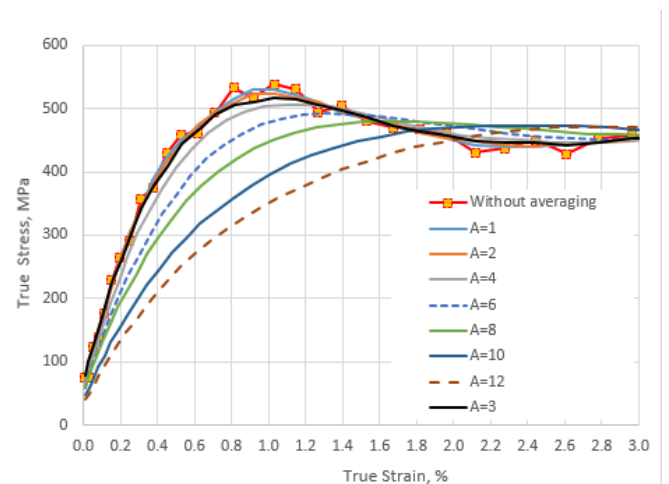


Fig. 6 Test sample diagrams, calculated in Excel when smoothing signals with different averaging amplitudes.

From Fig. 6 it is clear that the smoothing of the registered signals by averaging also leads to smoother diagrams and a decrease in the slope and height.

When averaging with an amplitude of 3 μs , the elastic modulus is obtained 6% smaller and the upper yield strength is obtained 4% smaller compared to the same indicators, determined without averaging the signals.

Averaging with an amplitude of 6 μs is similar to filtering with a 40 kHz cut-off frequency.

5. Conclusions

The influence of the amount of smoothing of the registered signals on the calculated diagram of the test body was studied using a Hopkinson-Kolsky bar impact test. Two methods have been used to smooth the signals: a low-pass filtering built into the software and arithmetic mean averaging.

It is shown (Figs. 5 and 6) that stronger smoothing leads to more significant changes in the initial slope of the calculated diagrams. It was found that both methods, filtering with 40 kHz cut-off frequency and averaging with an amplitude of 6 μs , have similar effect over the stress-strain diagram.

We concluded that filtering with a cutting frequency of 60 to 80 kHz and averaging with an amplitude of 3 to 4 μs leads to sufficient smoothing and neglectable deviation from the original (unfiltered) diagram.

6. Acknowledgments

This report is a research result of project BG05M2OP001-1.001-0008 "National Center for Mechatronics and Clean Technologies", funded by the Operational Program "Science and Education for Smart Growth" 2014-2020, co-financed by the European Union through the European Fund for Regional Development.

The authors express their gratitude to Prof. Dr. Dora Karagiozova for her assistance in introduction to the field of studies using Split Hopkinson-Kolsky Bar device.

7. References

1. Z. Li, Y. Wang, X. Cheng, J. Liang, S. Li, *Mat. Sc. and Eng.: A*, Vol. **772**, 138700 (2020)
2. M. Sedighi, M. Khandaei, H. Shokrollahi, *Mat. Sc. and Eng.: A*, Vol. **527**, Issue 15, pp. 3521-3528 (2010)
3. T. Zhou, J. Wu, J. Che, Y. Wang, X. Wang, *Int. J. of Imp. Eng.*, Vol. **109**, pp. 167-177 (2017)
4. W. Wang, M. Li, C. He, X. Wei, D. Wang, H. Du, *Mater. & Des.*, Vol. **47**, pp. 510-521 (2013)
5. Q. Fu, M. Bu, W. Xu, L. Chen, D. Li, J. He, H. Kou, He Li, *Int. J. of Imp. Eng.*, Vol. **148**, 103763 (2021)
6. G. Liu, E. Bai, J. Xu, N. Yang, T. Wang, *Constr. and Build. Mater.*, Vol. **261**, 119995, (2020)
7. Y. Guo, S. Xiao, J. Zeng, Yu Zheng, X. Li, F. Liu, *Constr. and Build. Mater.* Vol. **260**, 120460 (2020)
8. J. Zhu, C. Sun, Z. Qian, J. Chen, *Eng. Fail. Anal.* Vol. **18**, Issue 7, pp. 1808-1817 (2011)
9. S. Cao, G. Xue, W. Song, Q. Teng, *Constr. and Build. Mater.*, Vol. **247**, 118537 (2020)
10. X. Chen, X. Shi, J. Zhou, E. Li, P. Qiu, Y. Gou, *Int. J. of Mining Sc. and Techn.*, Vol. **31**, Issue 3, pp. 387-399 (2021)
11. Z. Huang, L. Sui, F. Wang, S. Du, Y. Zhou, J. Ye, *Comp. Str.*, Vol. **244**, 112300 (2020)
12. S. Feng, Yu Zhou, Yu Wang, M. Lei, *Int. J. of Imp. Eng.*, Vol. **140**, 103558 (2020)
13. R. Zwiessler, T. Kenkmann, M. H. Poelchau, S. Nau, S. Hess, *J. of Str. Geol.*, Vol. **97**, pp. 225-236 (2017)
14. F. Wang, S. Liu, L. Cao, *J. of Str. Geol.*, Vol. **138**, 104095 (2020)
15. J. Chen, H. Wei, K. Bao, X. Zhang, Y. Cao, Y. Peng, J. Kong, K. Wang, *J. of Mat. Res. and Techn.*, Vol. **11**, pp. 170-179 (2021)
16. B. Nurel, M. Nahmany, N. Frage, A. Stern, O. Sadot, *Vol. 22*, pp. 823-833 (2018)
17. P. Golewski, T. Sadowski, A. Rusinek, *Mater. Today: PROCEED.*, Vol. **45**, Part 5, pp. 4275-4279 (2021)
18. B. Jia, A. Rusinek, R. Pesci, R. Bernier, S. Bahi, P. Wood, *Int. J. of Solids and Str.*, Vol. **204-205**, pp. 153-171 (2020)
19. Gilat, A., Schmidt, T.E. & Walker, A.L., *Exp. Mech.*, Vol. **49**, pp. 291-302 (2009)
20. M. Ruiz de Sotro, P. Longère, V. Doquet, J. Papasidero, *Int. J. of Plast.*, Vol. **134**, 102777 (2020)
21. W. Chen, Bo Song, *Split Hopkinson (Kolsky) bar. Design, Testing and Applications*, Springer, Boston, MA, ISBN 978-1-4419-7982-7 (2011), p. 388
22. Ramesh K.T. High Rates and Impact Experiments. In: *Sharpe W. (eds) Springer Handbook of Experimental Solid Mechanics*. Springer Handbooks. Springer, Boston, MA. pp. 929-960 (2008)